Article

Assessing the Alkyl Chain Effect of Ammonium Hydroxides Ionic Liquids on the Kinetics of Pure Methane and Carbon Dioxide Hydrates

Muhammad Saad Khan [1] [ID], Cornelius Borecho Bavoh [2,3] [ID], Mohammad Azizur Rahman [1], Bhajan Lal [2,3,*], Ato Kwamena Quainoo [4] and Abdulhalim Shah Maulud [3,5] [ID]

[1] Petroleum Engineering Department, Texas A&M University at Qatar, Doha PO Box 23874, Qatar; khansaaad@gmail.com (M.S.K.); mohammad.rahman@qatar.tamu.edu (M.A.R.)

[2] CO2 Research Centre (CO2RES), Universiti Teknologi PETRONAS, Perak 32610, Malaysia; bavohcornelius@gmail.com

[3] Chemical Engineering Department, Universiti Teknologi PETRONAS, Perak 32610, Malaysia; halims@utp.edu.my

[4] Petroleum Engineering Department, Universiti Teknologi PETRONAS, Perak 32610, Malaysia; hansona433@gmail.com

[5] Center of Contaminant Control & Utilization (CenCoU), Universiti Teknologi PETRONAS, Perak 32610, Malaysia

* Correspondence: bhajan.lal@utp.edu.my; Tel.: +60-53687619

check for updates

Abstract: In this study, four ammonium hydroxide ionic liquids (AHILs) with varying alkyl chains were evaluated for their kinetic hydrate inhibition (KHI) impact on pure carbon dioxide (CO_2) and methane (CH_4) gas hydrate systems. The constant cooling technique was used to determine the induction time, the initial rate of hydrate formation, and the amount of gas uptake for CH_4-AHILs and CO_2-AHILs systems at 8.0 and 3.50 MPa, respectively, at 1 wt.% aqueous AHILs solutions. In addition, the effect of hydrate formation sub-cooling temperature on the performance of the AHILs was conducted at experimental temperatures 274.0 and 277.0 K. The tested AHILs kinetically inhibited both CH_4 and CO_2 hydrates at the studied sub-cooling temperatures by delaying the hydrate induction time and reducing the initial rate of hydrate formation and gas uptake. The hydrate inhibition performance of AHILs increases with increasing alkyl chain length, due to the better surface adsorption on the hydrate crystal surface with alkyl chain length enhancement. TPrAOH efficiently inhibited the induction time of both CH_4 and CO_2 hydrate with an average inhibition percentage of 50% and 84%, respectively. Tetramethylammonium Hydroxide (TMAOH) and Tetrabutylammonium Hydroxide (TBAOH) best reduced CH_4 and CO_2 total uptake on average, with TMAOH and Tetraethylammonium Hydroxide (TEAOH) suitably reducing the average initial rate of CH_4 and CO_2 hydrate formation, respectively. The findings in this study could provide a roadmap for the potential use of AHILs as KHI inhibitors, especially in offshore environs.

Keywords: ammonium hydroxide ionic liquids (AHILs); CH_4 hydrate; CO_2 hydrate; alkyl chain; ionic liquids; kinetic hydrate inhibition (KHI)

1. Introduction

Clathrate hydrates generally form by the combination of hydrogen-bonded water (host) and gas molecules (<10 Å) at certain favourable thermodynamic conditions via van der Waals force of attractions [1]. Three types of hydrate structures exist depending on the size and shape of the guest: structure I (sI), structure II (sII), and structure H (sH). sI consist of 5^{12}(2) and $5^{12}6^2$(6) cages made

46 H_2O molecules, while sII forms $5^{12}(16)$ and $5^{12}6^2(8)$ with 136 H_2O molecules. sH has 34 H_2O molecules made of $5^{12}6^8(1)$, $4^35^66^3(2)$, and $5^{12}(3)$ cages [2]. Gas (guest) molecules (≥5 Å), like carbon dioxide (CO_2) and methane (CH_4), usually form sI hydrates, while larger guest molecules form either sII or/and sH hydrates [3]. Hydrate formation is a prime flow assurance problem encountered in the petroleum industry. Hydrate formation hinders hydrocarbon transportation, and this could stop production operations [4,5] and drilling activities [6–8]. Since petroleum exploration and production move towards deep offshore locations, the possibility of confronting hydrate formation risks is high due to the thermodynamically favourable conditions. Moreover, the co-existence CO_2 increases the system hydrate formation risk, due to its lower hydrate formation equilibrium pressure than CH_4. Therefore, hydrate mitigation strategies for both CO_2 and CH_4 are needed to provide safe hydrocarbon transportation in pipelines [9,10].

The oil and gas industry spends billions of dollars per year to combating hydrate formation via chemical inhibition [11,12]. The chemical inhibitors are classified into thermodynamic hydrate inhibitors (THIs) and low dosage hydrate inhibitors (LDHIs) [13]. THIs are mostly organic solvents and are highly volatile due to their vapor losses and environmental limitations [14,15]. Therefore, the industry is focused on risk management gas hydrate additives known as LDHIs. The LDHIs are further grouped into Anti Agglomerates (AAs) and kinetic hydrate inhibitors (KHIs). However, they are used in smaller quantities than THIs. KHIs are generally hydrophilic polymers in nature such as polyvinylpyrrolidone (PVP), which mainly delays hydrate nucleation time by intermingling at the hydrate-gas surface and, as a result, provide substantial steric hindrance amid the gas and water interface. The KHIs are ineffective at higher sub-cooling environments, which are mostly experienced in deeper water locations where elevated sub-cooling conditions could possibly lead to the catastrophic hydrate formation and growth [16]. Moreover, KHIs are not completely environmentally benign, thus, their applications are discouraged [17,18].

For that reason, the quest for innovative, environmentally friendly, non-volatile, and dual functional hydrate inhibitors, led to the introduction of ionic liquids (ILs). Xiao and Adidharma [19] reported imidazolium-based ILs (IMILs) as dual-functional gas hydrate inhibitors. There are several gas hydrate studies on IMILs [20–30]. However, the effect of different classes of ILs on gas hydrate formation is limited [23,26,31–34], especially ammonium based ILs (AILs) [35–40]. Keshavarz et al. [32] found that tetraethylammonium chloride (TEACl) was the best THI when compared with IMILs systems.

In other to evaluate the dual functional performance of AILs, Tariq et al. [41] investigated the different families of AILs at 1 wt.% and 5 wt.% for CH_4 hydrates. Their findings revealed that the dual functional ability of AILs is affected by their anion and alkyl chain length [41]. Moreover, in our earlier works, tetramethylammonium hydroxide (TMAOH) [40] and tetramethylammonium chloride (TMACl) [42] were also reported as suitable THIs for both CO_2 and CH_4 hydrate. Although there are several reported studies [23,36,41,43–46] on AILs' THI behaviour, their KHI performance is less reported in the literature. Most of the reported systems mainly dealt with the IMILs families, and few focused on the kinetic behaviour of AILs on CH_4 and CO_2 hydrates formation. Moreover, none of the prior discuss the impact of AHILs alkyl chain length on their KHI performance.

Thus, in this present work, an attempt is made to extend our previous work on mixed gases of CH_4 and CO_2 to their respective pure gas systems. Herein, the KHI evaluation of four Alkyl Hydroxide Ammonium Ionic Liquids (AHILs) on pure CH_4 and CO_2 gas hydrate systems is presented. The KHI impact of AHILs are evaluated at two different temperature conditions, (277.0 and 274.0 K) to study the sub-cooling effect at 1 wt.%, which could represent a moderate to high hydrate prone conditions. The selection of AHILs was done to allow the evaluation of their alkyl chain length effect. To evaluate the KHI performance of the AHILs in extreme environments, all the experiments are performed at high-pressure conditions of 8.0 and 3.50 MPa for CH_4 and CO_2 hydrates, respectively. Moreover, the experiments were further conducted with the commercial inhibitor (PVP) at high sub-cooling conditions, and the obtained results were compared with AHILs and other ILs systems for both studied

gaseous systems. The findings in this work would provide more insight into the implementation of ionic liquids as gas hydrate inhibitors in gas production and processing operations.

## 2. Materials and Methods

2.1. Materials

The tested chemicals (AHILs) were supplied by Merck milli-pore (Germany) and used without further purification, as outlined in Table 1. Deionized water was used to prepare the concentrations of AHILs solutions for all the studied samples. The CH_4 and CO_2 were purchased from Gas Walker Sdn. Bhd. (Malaysia).

Table 1. Chemicals used in this study.

No.	Chemical	Chemical Formula	Purity
1	Water	H_2O	Deionized
2	Methane	CH_4	99.995 mol%
3	Carbon Dioxide	CO_2	99.995 mol%
4	Tetramethylammonium Hydroxide	TMAOH	40 wt.% in aqueous solution
5	Tetraethylammonium Hydroxide	TEAOH	40 wt.% in aqueous solution
6	Tetrapropylammonium Hydroxide	TPrAOH	40 wt.% in aqueous solution
7	Tetrabutylammonium Hydroxide	TBAOH	25 wt.% in aqueous solution

2.2. Experimental Setup and Methods

The high-pressure volumetric equilibrium cell having a maximum capacity of 650 mL was used in this study. The apparatus can efficiently operate within the temperature and pressure ranges from 253.0 to 323.0 K and up to 20.0 MPa, respectively. Details about the equipment setup can be found in our earlier reported articles [9,35,40,47]. The setup has a PID controlled thermostat bath, which is used to control the temperature in the cell during experimentation. In addition, an upper and lower temperature sensor is installed in the cell to measure the cell temperature. A pitch impeller stirrer is used to provide enough mixing in the liquid phase at 400 rpm. The pressure in the cell is controlled and monitored with a pressure transducer of accuracy ± 0.01 MPa. The detailed schematic diagram of the apparatus is shown in Figure 1.
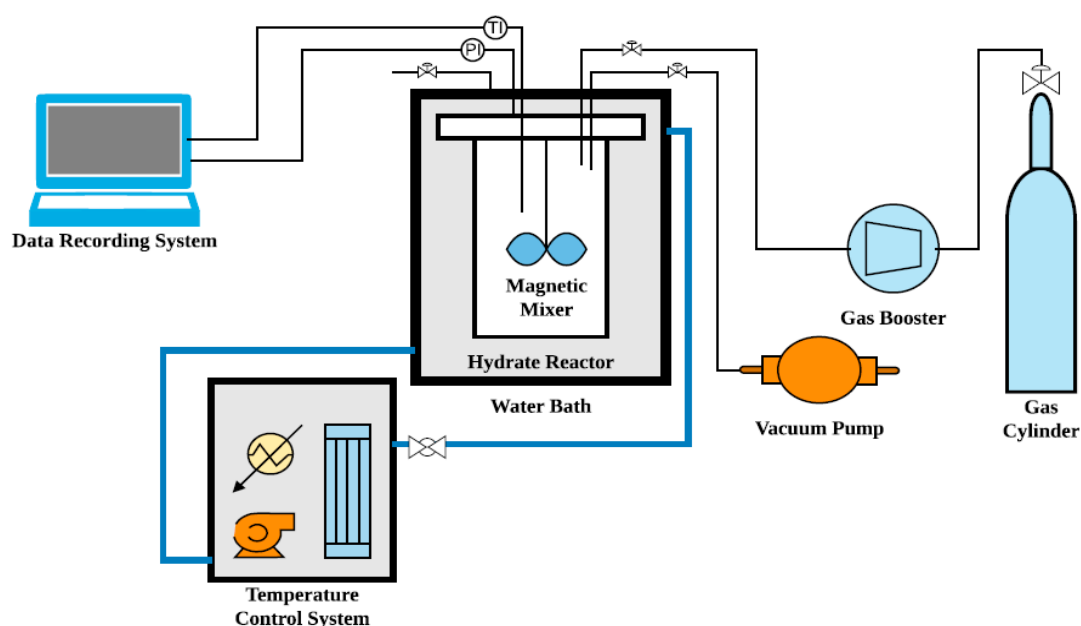

Figure 1. Schematic diagram of the experimental setup.

2.3. Kinetic Measurement Procedure

Table 2 presents the experimental kinetic details of gaseous systems together with the temperature and pressure conditions in the absence and presence of aqueous AHILs solutions. The KHI experimental testing pressures and temperature conditions were selected to represent the typical hydrate plugs challenges encountered in gas transmission lines. Additionally, to assess the effect of sub-cooling (driving force) on CH_4 and CO_2 hydrate formations, the KHI experiments were performed at two (2) different experimental temperatures of 274.0 and 277.0 K. In addition, the performance of the AHILs was compared with PVP at 1 wt.% at for both CO_2 and CH_4 hydrate systems.

An isochoric constant cooling technique was employed in all the kinetic experiments for KHI evaluation. Prior to all experimental runs, the cell is cleaned to remove contaminants, after which 100 mL of the AILs solution is poured into the hydrate cell. The hydrate cell is placed in the water bath and simultaneously placed on a vacuum. The target gas was then compressed to the necessary experimental running pressure inside the hydrate cell. Afterward, the system was left to stabilize by allowing it to cool for almost an hour to the appropriate initial test temperature and pressure limits. The stirrer is switched on at 400 rpm and the data logging program is begun continuously upon initiation of the experiment. The experimental testing pressure was 8.00 MPa for CH_4 and 3.50 MPa for CO_2 systems. All the systems were tested at 274.15 and 277.15 K and repeated thrice with their mean then presented. At the stage or time when there is constant pressure in the hydrate cell (for about five hours), the testing is terminated and considered complete, as illustrated in Figure 2. The observation of a sharp decrease in the system's pressure signifies the formation of hydrates.
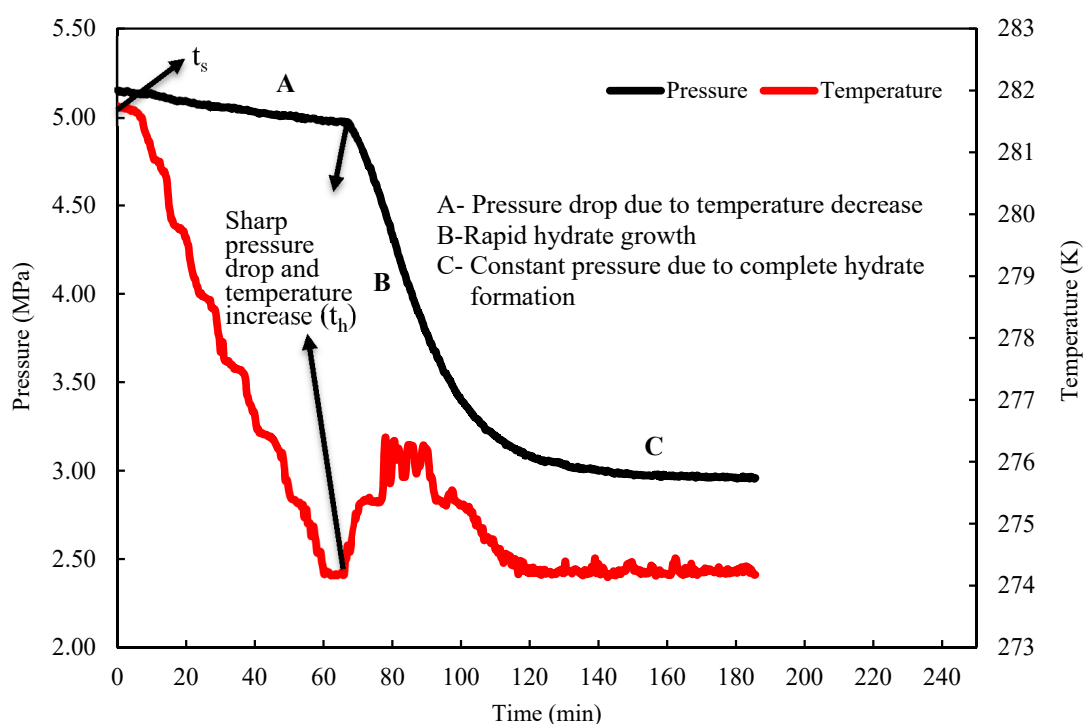
Figure 2. Pressure and Temperature—time plot recorded during hydrate formation testing.

Table 2. The details of hydrate testing experimental conditions.

Gas	Pressure Ranges (MPa)	Temperature (K)
CH_4	8.0	274.0 and 277.0
CO_2	3.50	274.0 and 277.0

2.4. Hydrate Kinetic Parameters

2.4.1. Nucleation/Induction Time

The time required for an additive to perform poorly, or for hydrate crystal to appear is called the hydrate nucleation time, t_i. The nucleation time in this study was calculated using the temperature/pressure versus time profile shown below (Figure 2) as

$$t_i = t_s - t_h, \tag{1}$$

where t_s is the time at initial hydrate testing conditions, and t_h is the time when hydrates began to form.

2.4.2. Total Gas (CH_4 and CO_2) Uptake

The total CH_4 and CO_2 uptake or moles consumed into hydrates were estimated by employing the real gas equation (see Equation (2)).

$$\Delta n_H = \left[\frac{PV}{zRT}\right]_0 - \left[\frac{PV}{zRT}\right]_t \tag{2}$$

where, T, P, V, z, and R are system temperature, pressure, gas-phase volume, compressibility factor, and the gas constant, respectively.

2.4.3. Initial Hydrate Formation Rate

The initial hydrate formation rate was determined using the description expressed in Equation (3) adopted from Nashed et al. [48].

$$rate = \frac{n_t - n_s}{dt} \tag{3}$$

where n_t is the moles of methane uptake converted to hydrate at time t of initial rapid hydrate growth with respect to the sharp pressure drop in the system, and n_s is the moles of methane uptake at induction time, and dt is the time difference between n_t and n_s.

2.4.4. Relative Inhibition Efficiency (RIE)

The relative inhibition efficiency (RIE) was determined to comparatively evaluate the inhibition efficiency of the kinetic inhibition parameters (induction time, methane uptake, and rate of hydrate formation) [14,17,42,49]. The values for RIE are calculated relative to pure water and AILs solution samples as fractional inhibition. Positive RIE values represent hydrate inhibition, whereas negative values present hydrate promotion. The RIE values for all the kinetic hydrate inhibition parameters were calculated using Equation (4).

$$RIE_{induction\ time} = \frac{Indution\ time_{inhibitor} - Indution\ time_{pure\ water}}{Indution\ time_{pure\ water}}, \tag{4}$$

3. Results and Discussion

3.1. Effect of AHILs on the Induction Time of CH_4 and CO_2 Hydrates

The kinetic formation measurements of CH_4 and CO_2 hydrates in the presence of AHILs were assessed at moderate experimental pressures (8.0 and 3.5 MPa) to evaluate their inhibition strength in simulated seabed sub-cooling conditions. Both the CH_4 and CO_2 hydrate systems were investigated at 277.0 and 274.0 K in the absence and presence of the AHILs to study the influence of sub-cooling on hydrate formation.

Figure 3 illustrates the effect of 1 wt.% AHILs on the average induction time of CH_4 hydrates at different experimental temperatures (277.0 and 274.0 K). The induction time of water (without AHILs)

was 29.8 min and 37.9 min at 274.0 and 277.0 K, respectively. The variation in the induction times was controlled by the different sub-cooling effect. Thus, hydrate formed faster in the system with a higher sub-cooling than the system with a lower sub-cooling degree.
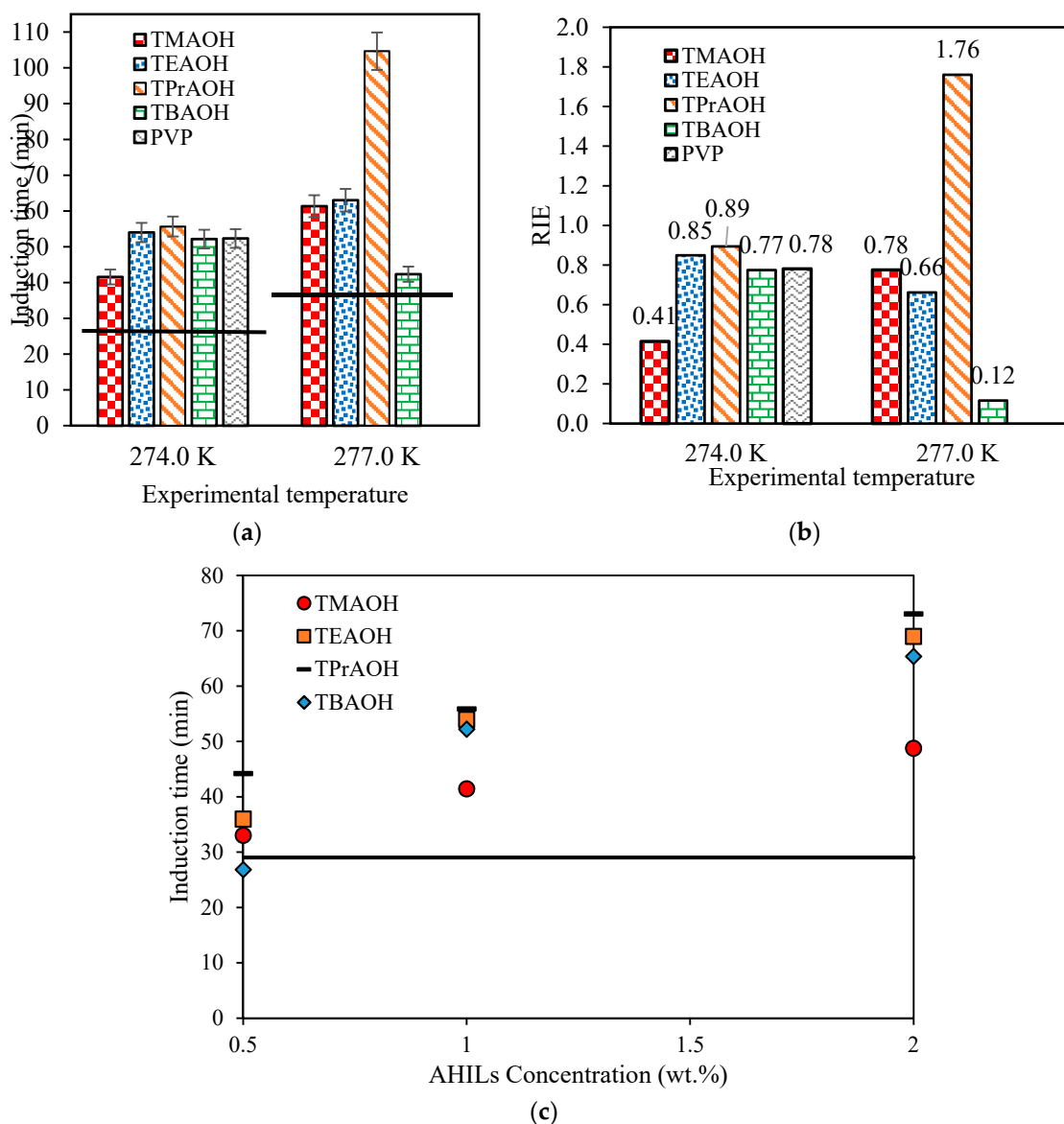
Figure 3. Effect of AHILs on the measured CH_4 hydrate induction times at different experimental temperatures at 1 wt.%: (**a**) Induction time at 274.0 and 277.0 K; (**b**) RIE for the CH_4 hydrate system; (**c**) Effect of AHILs concentrations on the methane hydrate formation induction time at 274.15 K; The black line symbolizes pure water values; No hydrate formation was observed for PVP at 277.0 K.

The measured average induction time of AHILs increases with the increasing alkyl chain length of their cations up to $TPrA^+$ (TMAOH < TEAOH < TPrAOH), then decreases in the presence of TBA^+ cation. Therefore, apart from TBAOH, the induction time of AHILs at 1 wt.% and 277.0 K was found in the following decreasing order: TPrAOH > TEAOH > TMAOH > TBAOH > water. It was expected that TBAOH should exhibit the best AHILs inhibitor to delay the CH_4 hydrate nucleation time because it has the longest alkyl chain, since longer chain ionic liquids are known to effectively inhibit hydrate formation [50]. However, TBAOH trail as the best inhibitor compared with the other AHILs because of its long carbon chain causing the formation of micelles within the studied concentration range. According to Tariq et al. [41], ammonium-based ILs with longer chains (>C3) have the tendency to

form micelles at low concentrations (≤2 wt.%) in aqueous solution. These micelles act in a mild surfactant nature to slightly prevent aggregation at the gas/liquid interface for CH_4 hydrate systems, which reduces the inhibition strength of the chemical (TBAOH). Though the inhibition impact of TBAOH in Figure 3 slightly increases with concentration, the presence of micelles formation reduces its performance compared with the other tested AHILs at all concentrations. The micelles formations in the TBAOH aqueous systems were considered as mild for all the tested concentrations (≤2 wt.%) in this study, as suggested by Tariq et al. [41]. However, it can be observed in Figure 3 that the inhibition strength of TBAOH retards with concentration as compared with other AHILs. For example, at 1 wt.% the CH_4 hydrate inhibition impact is about 73%. When the concentration is doubled (2 wt.%), the induction time inhibition impact further increased by only 43%. This decrease in inhibition strength with concentration could probably be due to the mild system micelle formation and/or the hydrate nuclei crystallization orientation with the aqueous TBAOH solution [51]. Further studies on the effect and quantification of micelles formation of AILs with varying concentrations on CH_4 hydrates are recommended.

In addition, the subcooling effect on TBAOH is found to be unusual with regards to its induction time and rate of hydrate formation. The induction time and rate of hydrate formation (Figures 3–6) of CH_4 hydrate are high at 277 and lower at 274 K. In both systems, the TBAOH micelle formation behavior affects the surface activity of the system via the reduction of the hydrophilic effect of the system, as discussed by Zielinski et al. [52]. This guarantees the possibility of hydrate forming during the cooling stage for both systems based on the complex nucleation stochasticity of hydrate formation. It must be stated that, for most of the system in this work, the onset of hydrate formation occurs during the constant cooling stage before reaching the experimental temperatures, which in effect could initiate the hydrate formation arbitrary once the meta-stability in either systems is overcome in the hydrate stability region as cooling continues. Hence, the varying inhibition effect at different experimental temperatures is mainly attributed to the nucleation probabilistic effect, which is described by Sowa et al. [51], has been solely system dependant, i.e., gas type, concentration and temperature dependant. However, it is also possible that the system cooling rate might lead to such an unusual nucleation phenomenon [53]. Subsequently, the gas dissolution in the lower subcooling system might be undersaturated and delay its hydrate formation time as compared to the higher subcooling system.

The impact of the AHILs on the induction time of CH_4 hydrate at higher sub-cooling temperature 274.0 K (higher sub-cooling = 10.8 K) confirms their hydrate inhibition potentials in Figure 3a. Interestingly, the induction time delaying ability of the AHILs for CH_4 hydrate at 274 K was similar to PVP (commercial KHI). The measured induction time of all the AHILs were less at a high sub-cooling temperature (274.0 K) compared to the lower sub-cooling condition (277.0 K), except for TBAOH. The presence of a strong driving force at high sub-cooling explains the short hydrate nucleation time at 274.0 K. At the 274.0 K condition, the induction times of AHILs are established in a following decreasing orders: TPrAOH > TEAOH > PVP > TBAOH > TMAOH > water. Results also suggested that the KHI performance is immensely dependant on the structure of the AHILs. It had been reported earlier in the literature that the longer alkyl chain cations enhance the kinetic hydrate inhibition effect more than the shorter ones (for instance, $[BMIM]^+$ exhibited better kinetic inhibition than $[EMIM]^+$) [23]. Nashed et al. [54] reported a similar trend when they studied the KHI behaviour of imidazolium-based ILs by varying their alkyl chains. They reported that an increasing IL alkyl chain improves gas hydrate formation nucleation time. However, in the case of ammonium salts, a chain length increment above $TPrA^+$ results in the formation of micelles at low concentrations, thus, causing the induction time of TBAOH to be less as expected.

Moreover, the kinetic inhibition of the anion is also evident in the comparison between TMACl [42] and TMAOH. At a higher sub-cooling condition (274.0 K), TMAOH (41.55 min) delays hydrate formation nucleation time more efficiently than TMACl (31.25 min). This enhanced inhibition of TMAOH over TMACl is probably due to the ability of the OH^- functional group to form hydrogen bond cleavages owing to its high hydrogen bonding affinity with water molecules [23]. The hydrogen-bonded

network slightly stemmed from the sub-cooling temperature resulted in a lowered driving force, thus shelving hydrate formation.

The relative inhibition efficiency (RIE) values in Figure 3b quantitatively confirm the kinetic inhibitory efficacy of the tested AHILs. Koh and coworkers [55] proposed a method known as the relative inhibition efficiency (RIE), which could be used to effectively compare the kinetic hydrate inhibition impact of different kinds of systems independent of their experimental conditions. RIE values greater than zero (0) denote the superior inhibitory performance of the KHIs. The RIE data of the AHILs at different experimental conditions are presented in Figure 3b. The RIE results add more clarity to the KHI performance of the AHILs. The effect of sub-cooling was also evident in the RIE attained data. For instance, the RIE of the AHILs is lower at a higher sub-cooling condition (274.0 K), than a lower sub-cooling condition (277.0 K). This is due to the existence of high hydrate formation driving forces induced by the higher sub-cooling temperature at 274.0 K. The KHI performance (RIE) of TPrAOH (0.89) appears to be superior to the PVP (0.78) (commercial KHI). Furthermore, RIE data of considered AHILs were compared with previous studies (with a different class of ILs), as reported by Nashed et al. [54] and Khan et al. [42] in Table 3. All the considered AHILs possess better RIE values than the earlier imidazolium-based ILs studied by Nashed et al. [54].

Table 3. The comparisons of RIE data for 1 wt.% CH_4/CO_2 -ILs system.

Author	Studied System	RIE	
		CH_4	CO_2
Nashed et al. [54]	[BMIM][CF$_3$SO$_3$]	0.35	-
Nashed et al. [54]	[BMIM][CH$_3$SO$_4$]	0.39	-
Nashed et al. [54]	[OH-EMIM] [Br]	0.45	-
Chun et al. [12]	[EMIM][BF$_4$]	-	0.27
Bavoh et al. [56]	[EMIM][Cl]	-	1.06
Khan et al. [42]	TMACl	0.063	2.0
This study	TMAOH	0.41	0.30
This study	TEAOH	0.85	1.00
This study	TPrAOH	0.89	3.50
This study	TBAOH	0.77	3.80
This study	PVP	0.78	1.90

Figure 3c illustrates the influence of the AHILs concentration on the induction time of CH_4 hydrate. From the induction time data, it can be deduced that almost all the studied AILs systems (except 0.5 wt.% TBAOH) increase the methane hydrate formation induction time with an increasing concentration. This suggests that the hydrate delay (nucleation) seems to be concentration dependent. The improved inhibition performance is found to be attained with increased AHIL concentrations, perhaps attributed due to the enhanced activity of water and AHILs solutions (with increases AHILs concentrations). Therefore, considering Figure 3, TPrAOH was the best KHI inhibitor at all studied concentrations among the AHILs. The reason for improved KHI inhibition of TPrAOH is perhaps due to the optimum alkyl chain length, which can provide sufficient adsorption on gas–liquid and hydrate–gas interfaces together with proficient hydrogen bonding ability to hinder the hydrate formations [57]. The kinetic hydrate inhibition impact is concentration and guest (gas) molecule type dependent [42,51]. Hence, the hydrate inhibition effect on CO_2 was different for CH_4. The formation pressure of CO_2 hydrates is significantly less compared to CH_4 hydrates due to the bigger diameter size of CO_2 (CO_2 = 5.12 Å or CH_4 = 4.36 Å) [58] together with the higher solubility of CO_2 in water [42,59], making CO_2 prone to hydrate formation.

The average induction time of AHILs on CO_2 hydrates for 1 wt.% concentration at different experimental temperature conditions at 274.0 and 277.0 K is presented in Figure 4. CO_2 generally form hydrates quite fast compared to the CH_4 hydrates at the same experimental temperature conditions, owing to proneness to hydrate formation at smaller driving forces [17,42]. The average induction time

of CO_2 hydrates without AHILs is found to be 12.35 and 14.35 min at 277.0 and 274.0 K temperatures, respectively. The extent of AHILs' kinetic inhibition on CO_2 hydrates is different from CH_4 hydrates, as observed in Figures 3 and 4. This means that inconsistent inhibition trends for hydrate nucleation time exist between CH_4 and CO_2 hydrates in the presence of AHILs, thus, suggesting the effect of guest (gas) molecule type on the kinetics of hydrate formation [51]. These findings are consistent with Sowa et al. [51] who indicated that hydrate nucleation or kinetics are greatly influenced by the guest or gas molecule type. Therefore, based on the type of gas and chemical, the hydrate inhibition mechanism could either be via surface adsorption [55] or crystal perturbation activities by a hydrogen bonding effect [60]. For instance, TBAOH in the CH_4 system performs relatively less compared with other AHILs (see Figure 3) because of its micelles formations behavior which reduces its surface activity causing the enhancement of CH_4 dissolution into the liquids phase, thus reducing its performance. However, in the presence of polar gases, such as CO_2, which could possibly interact with aqueous TBAOH solution, leads to the perturbation of the water structures and delay hydrate nucleation (see Figure 4). According to Zielinski et al. [52], the formation of micelles in ammonium salts favors their hydrophilic effect, which enables them to perturb the local water structure via hydrogen bonding; this then causes the nucleation process in the CO_2 system to increase more than in the CH_4 system [60]. On the contrary, in the CH_4 system a strengthened hydrophilic surface of the TBAOH solutions affects their hydrophobic shield which weakens the gas/liquid interface and causes a favorable CH_4 dissolution in the liquid phase and reduces the hydrate inhibition impact of TBAOH.

Among the tested AHILs aqueous solutions, TBAOH was the most effective kinetic inhibitor in both experimental conditions at 1 wt.%. All the AHILs could prolong the induction time. In the presence of the CO_2 hydrates at 277.0 K, the induction times of AHILs are in the increasing order of water < TMAOH < TEAOH < TPrAOH < TBAOH at 1 wt.%.

At 274.0 K, the induction times of CO_2-AHILs are reduced when compared to the 277.0 K experimental condition. The induction time delays for CO_2 hydrates at 274 K are in an increasing order, as follows: water < TMAOH < TEAOH < PVP < TPrAOH < TBAOH. The AHILs with longer alkyl chains (TBAOH, TPrAOH) prolong CO_2 hydrates inhibition similar to the CH_4 system; however, there is no critical inhibition chain length for the AHILs in CO_2 hydrate system at 1 wt.%. A comparison between studied anions (OH^- and Cl^-) for CO_2 hydrates, TMACl [42] (42.6 min) provide better induction time inhibition than TMAOH (19.0 min) potentially, due to the better surface adsorption of Cl^- on the surface of the water, as mentioned by the earlier study [56].

Table 3 shows the RIE results studied for 1 wt.% CO_2-ILs systems. At lower temperature conditions (274.0 K), the KHI impact (RIE) of longer alkyl chain AHILs (TBAOH (3.8) and TPrAOH (3.5)) was found to be superior to the PVP (1.9) (commercial KHI). Moreover, RIE data of studied AHILs are comparable with prior studies like Chun et al. [12], Bavoh et al. [56], and Khan et al. [42] as shown in Table 3. In fact, most of the considered AHILs (TEAOH, TPrAOH, and TBAOH) possess better RIE values compared to the earlier studied ILs systems. In the case of hydroxyl anions (OH^-), the influence of the alkyl chain can also be observed from the induction time data at 277.0 K. With an increase in the AHILs alkyl chains; the induction time is enhanced. This is due to the better adsorption of the cation at the surface of the gas–liquid and hydrate–liquid interface, reducing the dissolution of gas into the liquid phase [61].

The RIE results of AHILs at lower sub-cooling (277.0 K) temperature show higher RIE values at lower sub-cooling than higher sub-cooling temperature (274.0 K) owing to the less significant driving force (see Figure 4b). The RIE values at lower sub-cooling were related to the alkyl chain of the AHILs [14,42,62,63]. In Table 3, the induction time inhibition performance of AHILs is more evident and effective in the CO_2 hydrate system compared with CH_4. In addition, the hydrate induction time inhibition time is delayed more as AHILs concentrations increase in both CH_4 and CO_2 hydrate systems.
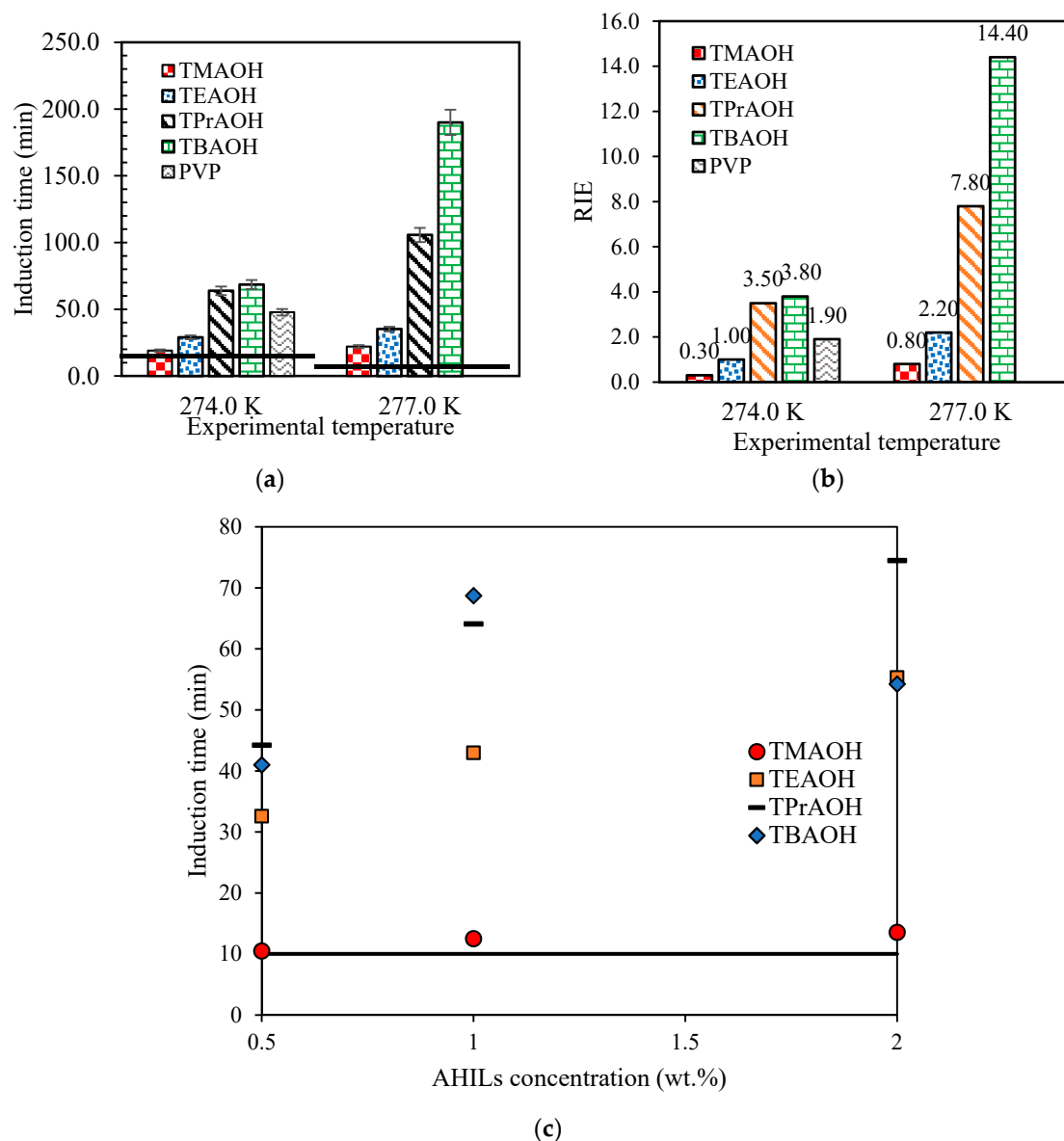
Figure 4. Effect of AHILs on the measured CO_2 hydrate induction times at different experimental temperatures at 1 wt.%: (**a**) Induction time at 274.15 and 277.15 K; (**b**) RIE for CO_2 hydrate system; (**c**) Effect of AHILs concentrations on the CO_2 hydrate formation induction time at 274.15 K; The black line symbolizes pure water values; No hydrate formation was observed for PVP at 277.0 K.

3.2. Effect of AHILs on the Initial Formation Rate of CH₄ and CO₂ Hydrates

According to Sloan and co-workers [58], hydrate crystal growth periods (initial formation rates) are technically more rational than induction time information due to the intricacy of the hydrate nucleation process. The rate of hydrate formation of CH_4 and CO_2 hydrate in the presence of 1 wt.% AHILs at different experimental temperatures (274.0 and 277.0 K) are considered and reported in Figure 5a.
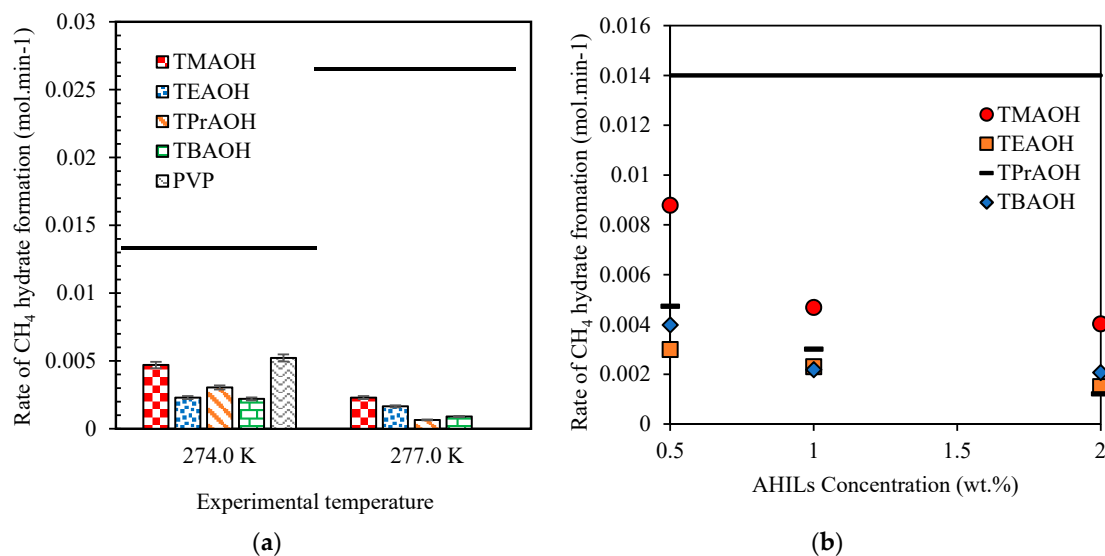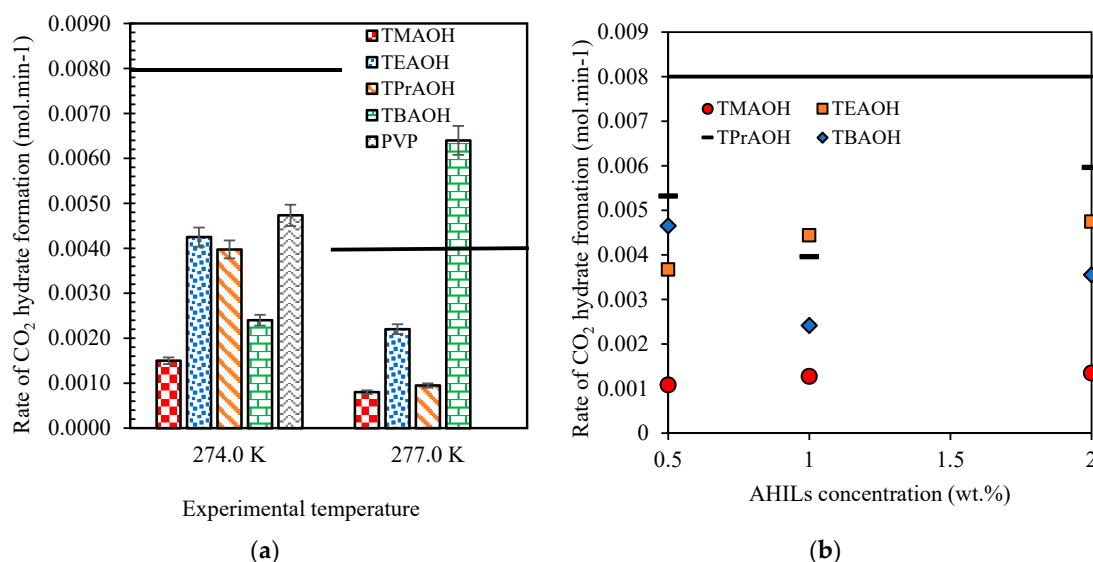
Figure 5. (**a**) Effect of AHILs on the measured CH_4 hydrate initial rate of formation at different experimental temperatures at 1 wt.%; (**b**) Effect of AHILs concentrations on the CH_4 hydrate initial rate of formation at 274.15 K; The black line symbolizes pure water values; No hydrate formation was observed for PVP at 277.0 K.

The estimated initial formation rate of pure water for CH_4 hydrates is 0.015 and 0.0276 mol·min^{-1} at 274.0 and 277.0 K conditions, respectively. However, in the CO_2 hydrate system, the initial formation rate was 0.0042 and 0.0079 mol·min^{-1} for 274.0 and 277.0 K, respectively. For lower sub-cooling temperature conditions (277.0 K and 1 wt.%), all the studied AHILs significantly reduce the initial formation rate of CH_4 hydrates compared with water. The initial formation results further confirmed the superior kinetic performance of TPrAOH, which exhibits the lowest CH_4 hydrate formation rate among all considered AILs at 277.0 K and 1 wt.%. The initial formation rates of the studied AHILs (at 277.0 K) are in the following increasing order: TPrAOH < TEAOH <TBAOH < TMAOH < water for CH_4 hydrates (see Figure 5a). However, in CO_2 hydrates, TBAOH trailed to inhibit the initial formation rates, thus, in CO_2-AHILs hydrates (at 277.0 K) the following increasing order of hydrate inhibition was observed: TMAOH < TPrAOH < TEAOH < water < TBAOH (Figure 6).

Furthermore, the initial formation rate of AHILs is also reported at higher sub-cooling ($\approx$ 10.8 K) at 274.0 K experimental temperature and compared with water and commercial kinetic inhibitor, PVP. The initial formation rate of pure water is around 0.015 mol·min^{-1} at 274.0 K. The presence of all the AHILs solutions at 1 wt.% could reduce the methane hydrate formation rate (see Figure 5a). TEAOH and TBAOH reduced the methane rate of hydrate formation to about 0.0022 mol·min^{-1} at 1 wt.% and 274.0 K. However, the initial formation rates of AHILs were significantly reduced at the 277.0 K temperature compared to the 274.0 K temperature condition for both CH_4 and CO_2 systems due to the presence of higher driving force (sub-cooling) which causes rapid hydrate crystal growth at 274.0 K. The initial rate of CH_4 hydrate formation in AHILs solutions at 1 wt.% and 274.0 K are found to be in the following increasing order: TBAOH < TEAOH < TPrAOH < TMAOH < PVP < water (Figure 5a). The increment in the AHILs alkyl chain decreased the formation rates. The reason behind this is that, when the chain length of AHILs increases, the Van der Waals forces in the system are also intensified, hence strong interactions occur between the aqueous gas–liquid interfaces [17,64], which provides a reduced rate of hydrate formation on methane hydrates. All the AHILs inhibited the methane hydrate growth rate better than PVP at 1 wt.% and 274.0 K. In Figure 5b, the presence of all the AHILs reduced the initial rate of hydrate formation with increasing concentration for CH_4 hydrates, perhaps due to the enhanced activity of AHILs with an increasing concentration.

However, for the CO_2 hydrate system (Figure 6b), the initial rate of CO_2 hydrate formation increases with concentration for TMAOH and TEAOH. TPrAOH and TBAOH showed their optimum

inhibition performance at 1 wt.%. The initial CO_2 hydrates formation rates in the tested AHILs solutions at higher sub-cooling conditions (10.8 K and 1 wt.%) are found to be following a decreasing order: water > PVP > TEAOH > TPrAOH > TBAOH > TMAOH as shown in Figure 6a. All the considered AHILs could reduce the initial formation rates of CO_2 hydrate better than PVP at 1 wt.%. Again, the anomaly behaviour of TBAOH as observed in Figure 6a is because of its micelles formation surfactant nature on the rate of CO_2 hydrate formation. Thus, causing the initial rate of hydrate growth to occur within a shorter time period (with high rate of formation) at 277.0 K than at 274.0 K in the presences of 1 wt.% TBAOH.
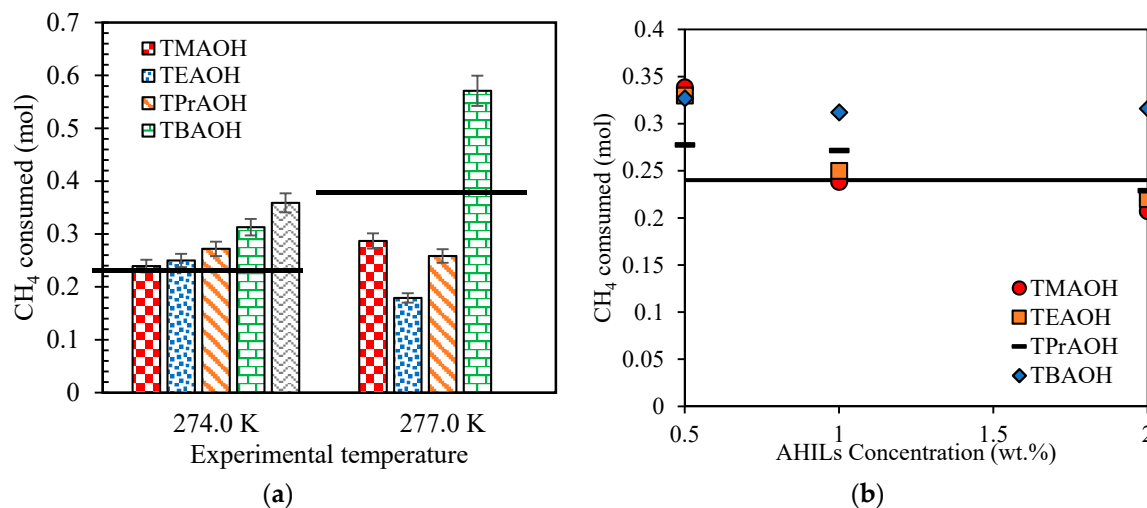

Figure 6. (**a**) Effect of AHILs on the measured CO_2 hydrate initial rate of formation at different experimental temperatures at 1 wt.%; (**b**) Effect of AHILs concentrations on the CO_2 hydrate initial rate of formation at 274.15 K; The black line symbolizes pure water values; No hydrate formation was observed for PVP at 277.0 K.

3.3. Effect of AHILs on Mole Consumption of CH_4 Hydrates

The total gas consumed or uptake defines the maximum amount of gas (moles) trapped into the hydrate lattice structure. Figure 7a shows the effect of AHILs on CH_4 uptake during the hydrate formation in this work. The obtained results at 277.0 K experimental temperature indicated that, apart from TBAOH, all AHILs reduce the overall methane hydrate mole consumption into hydrates. Since all the tested AHILs have the same anion (OH^-), the effect of their cation chain length causes their effects on the hydrate formation uptake. TEAOH exhibited the least moles of methane hydrate consumption due to the presence of TEA^+ cations (at 277.0 K and 1 wt.%). However, TBAOH significantly enhanced/promoted the overall methane hydrate moles consumption, due to its surfactant nature resulting from its micelles formation tendency. Therefore, this provides a positive guest dissolution into the liquid phase to form more hydrates [41,51]. Interestingly, hydrate formation was not observed in the presence of PVP after 48 h of experimentation at 277.0 K and 1 wt.%. This indicates that AHILs are poor inhibitors compared with PVP at lower sub-cooling degrees with 7.8 K. Additionally, the mole consumptions of methane hydrate with AHILs are reported at a lower temperature condition (274.0 K; sub-cooling = 10.8 K) and also compared with pure water and PVP (commercial KHI) samples. At higher sub-cooling, the mole consumption of CH_4 hydrates is not significantly affected by AHILs. With the increasing alkyl chain of AHILs, the CH_4 hydrate mole consumption is found to be increased at 1 wt.%. However, results revealed that all the studied AHILs have lower mole consumptions compared with PVP, which exhibited the highest CH_4 moles uptake. Similar behaviour was also reported by Nguyen et al. [57] for PVP, and they indicated that when PVP forms hydrate, it increases the total methane consumption, hence, behaving as a hydrate total uptake promoter. In Figure 7b, the

total methane uptake in hydrate formation is reduced with increasing AHILs concentrations. TMAOH had the best CH_4 mole uptake at 1 and 2 wt.%; however, at 0.5 wt.%, all the AHILs showed methane hydrate promotional effect. For the CO_2 hydrate system, the presence of AHILs shows an inconsistent relationship between the CO_2 moles consumed with concentration, indicating the dependence of hydrate inhibition of AHILs on concentration and guest molecule type as shown in Figures 7b and 8b.

Figure 7. (**a**) Effect of AHILs on the measured CH_4 consumed moles at different experimental temperatures at 1 wt.%; (**b**) Effect of AHILs concentrations on the CH_4 consumed moles at 274.15 K; The black line symbolizes pure water values; No hydrate formation was observed for PVP at 277.0 K.

The mole consumption of carbon dioxide hydrates is comparatively lesser than methane hydrates due to the moderate experimental pressure (3.50 MPa) used for the CO_2 hydrates systems. The influence of 1 wt.% AHILs (aqueous solutions) on the mole consumption of CO_2 hydrates are presented in Figure 8a. The results revealed that AHILs do not significantly inhibit CO_2 mole consumption at both experimental temperatures. TMAOH and TBAOH inhibited the CO_2 hydrate formation total uptake in both experimental conditions (at 274.0 K and 1 wt.%). However, TMAOH showed the best CO_2 moles uptake inhibition. All the remaining AHILs showed a CO_2 hydrate total uptake promotional effect, as shown in Figure 8a. The increase in mole consumptions of ammonium-based ionic liquids in CO_2 hydrates agree with the findings of Cha and coworkers [16], who reported that the presence of AILs prolongs the induction time of CO_2 hydrates to an extent which allows significant hydrate nucleation sites in the system. This causes more CO_2 to be consumed into hydrates once they begin to form (when the AILs inhibitor fails). A similar hydrate uptake promotional effect is exhibited by some commercial hydrate inhibitors like PVP.

The CO_2 moles' consumption data of AHILs at different concentrations illustrate that, at a lower strength, the mole consumption of CO_2 is reduced for all the studied concentrations (Figure 8b). Overall, TMAOH exhibited the least CO_2 uptake amongst the studied systems for all concentrations. The finding of this study suggested that the studied AHILs possess KHI abilities. Similarly, our earlier studies [9,14,15,65,66] have indicated that these AILs also possess good THI potential, which makes them potential dual-functional gas hydrate inhibitors. However, the THI and KHI properties are highly dependent on their effective alkyl chain length selection [14,42]. Therefore, to get better dual-functional performance, the appropriate chain length of ILs is essential. This study has shown that the use of AILs can be used as efficient gas hydrate inhibitors in flow assurance applications.
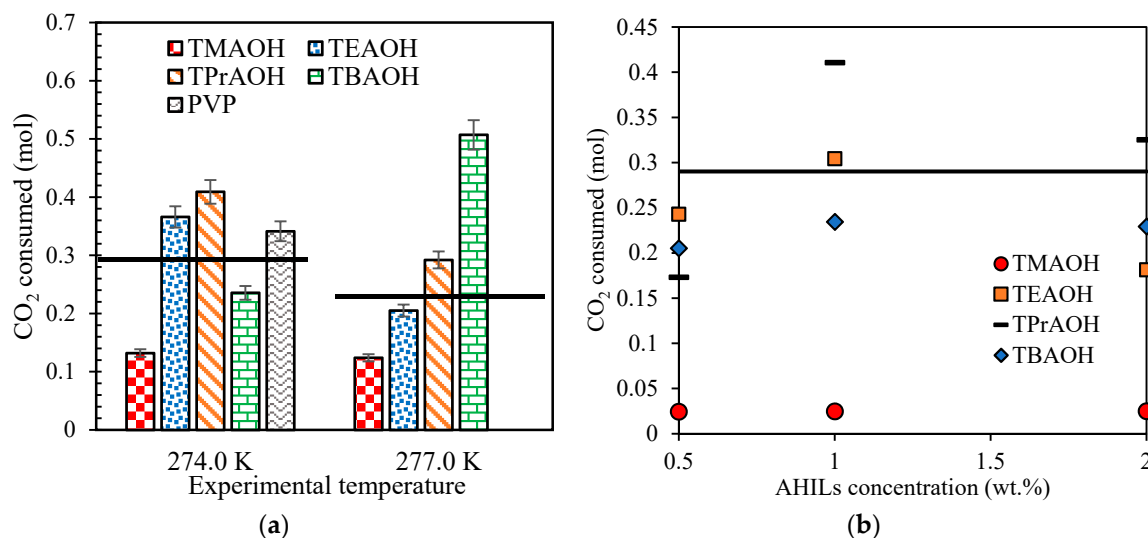
Figure 8. (**a**) Effect of AHILs on the measured CO_2 consumed moles at different experimental temperatures at 1 wt.%; (**b**) Effect of AHILs concentrations on the CO_2 consumed moles at 274.15 K; The black line symbolizes pure water values; No hydrate formation was observed for PVP at 277.0 K.

4. Conclusions

In this work, the formation kinetics of CH_4 and CO_2 gas hydrates in the presence of four AHILs are reported via a constant cooling approach at 1 wt.%. It was found that the presence of longer alkyl chain AHILs performed better in delaying CH_4 and CO_2 hydrate nucleation time and reducing their initial hydrate formation rate and gas uptake. TBAOH and TPrAOH were the best performing AHILs, and their inhibition impact was comparable to PVP (a commercial gas hydrate inhibitor). As the AHILs alkyl chain length increases, their surface adsorption affinity is enhanced, hence, providing more adsorption affinity on the hydrate crystal lattices. This causes the AHILs to inhibit the hydrate crystal nucleation and growth. Moreover, the formation kinetic results suggested that the KHI impact is concentration dependent. As the AHILs concentration increases, their inhibition impact is increased, especially in CH_4 hydrates systems. In addition, the hydrate inhibition effect of the studied AHILs strongly depends on the concentration, the guest molecule present, and the sub-cooling degree. However, the studied AHILs could inhibit the induction time and hydrate formation rate more than the total gas uptake.

Author Contributions: Conceptualization, M.S.K.; Formal analysis, M.S.K.; Funding acquisition, B.L., M.A.R.; Investigation, M.S.K.; Methodology, M.S.K. and C.B.B.; Resources, M.A.R.; Supervision, B.L.; Writing—original draft, M.S.K., C.B.B.; Writing—review & editing, C.B.B., A.K.Q., M.A.R. and A.S.M. All authors have read and agreed to the published version of the manuscript.

Conflicts of Interest: The authors declare no conflict of interest.

Abbreviations

AILs	Ammonium based Ionic liquids
AHILs	Ammonium Hydroxide Ionic liquids
[BMIM][BF$_4$]	1-butyl-3-methyl imidazolium tetrafluoroborate
CH$_4$	Methane
CO$_2$	Carbon Dioxide
DFIs	Dual-functional Inhibitors
EMIM-CL	1-ethyl-3-methyl imidazolium chloride
[EMPip[[Br]	N-ethyl-N-methyl piperidinium bromide

[EMPip][BF$_4$]	N-ethyl-N-methylpiperidinium tetrafluoroborate
[EMMor][BF$_4$]	N-ethyl-N-methylmorpholinium tetrafluoroborate
IMILs	Imidazolium Ionic Liquids
KHIs	kinetic hydrate inhibitors
LDHIs	Low dosage hydrate inhibitors
TBAOH	Tetrabutylammonium hydroxide
THIs	Thermodynamic hydrate inhibitor
TPrAOH	Tetrapropylammonium hydroxide
TMAOH	Tetramethylammonium hydroxide
TMACl	Tetramethyl ammonium chloride
TEAOH	Tetraethylammonium hydroxide

References

1. Bavoh, C.B.; Lal, B.; Osei, H.; Sabil, K.M.; Mukhtar, H. A review on the role of amino acids in gas hydrate inhibition, CO$_2$ capture and sequestration, and natural gas storage. *J. Nat. Gas Sci. Eng.* **2019**, *64*, 52–71. [CrossRef]

2. Ripmeester, J.A.; Tse, J.S.; Ratcliffe, C.I.; Powell, B.M. A new clathrate hydrate structure. *Nature* **1987**, *325*, 135–136. [CrossRef]

3. Khan, M.S.; Bavoh, C.B.; Lal, B.; Keong, L.K.; Mellon, N.B.; Bustam, M.A.; Shariff, A.M. Application of electrolyte based model on ionic liquids-methane hydrates phase boundary. *IOP Conf. Ser. Mater. Sci. Eng.* **2018**, *458*. [CrossRef]

4. Taylor, C.E.; Kwan, J.T. *Advances in the Study of Gas Hydrates*, 1st ed.; Kluwer Academic Publishers: Berlin/Heidelberg, Germany, 2004; ISBN 0-306-48645-8.

5. Zanota, M.L.; Dicharry, C.; Graciaa, A. Hydrate plug prevention by quaternary ammonium salts. *Energy Fuels* **2005**, *19*, 584–590. [CrossRef]

6. Bavoh, C.B.; Ofei, T.N.; Lal, B.; Sharif, A.M.; Shahpin, M.H.B.A.; Sundramoorthy, J.D. Assessing the impact of an ionic liquid on NaCl/KCl/polymer water-based mud (WBM) for drilling gas hydrate- bearing sediments. *J. Mol. Liq.* **2019**, 100820. [CrossRef]

7. Bavoh, C.B.; Yuha, Y.B.; Tay, W.H.; Ofei, T.N.; Lal, B.; Mukhtar, H. Experimental and Modelling of the impact of Quaternary Ammonium Salts / Ionic Liquid on the rheological and hydrate inhibition properties of Xanthan gum water-based muds for Drilling Gas Hydrate-Bearing Rocks. *J. Pet. Sci. Eng.* **2019**, 106468. [CrossRef]

8. Bavoh, C.B.; Ofei, T.N.; Lal, B. Investigating the Potential Cuttings Transport Behavior of Ionic Liquids in Drilling Mud in the Presence of sII Hydrates. *Energy Fuels* **2020**, *34*, 2903–2915.

9. Khan, M.S.; Bavoh, C.; Partoon, B.; Lal, B.; Bustam, M.A.; Shariff, A.M. Thermodynamic effect of ammonium based ionic liquids on CO$_2$ hydrates phase boundary. *J. Mol. Liq.* **2017**, *238*, 533–539. [CrossRef]

10. Bavoh, C.B.; Khan, M.S.; Ting, V.J.; Lal, B.; Ofei, T.N.; Ben-Awuah, J.; Ayoub, M.; Shariff, A.B.M. The Effect of Acidic Gases and Thermodynamic Inhibitors on the Hydrates Phase Boundary of Synthetic Malaysia Natural Gas. *IOP Conf. Ser. Mater. Sci. Eng.* **2018**, *458*, 012016. [CrossRef]

11. Patel, Z.D.; Russum, J. Flow assurance: Chemical inhibition of gas hydrates in deepwater production systems. *Multi-Chem* **2009**, *4*, 70–72.

12. Chun, L.K.; Jaafar, A. Ionic liquid as low dosage hydrate inhibitor for flow assurance in pipeline. *Asian J. Sci. Res.* **2013**, *6*, 374–380. [CrossRef]

13. Nasir, Q.; Lau, K.K.; Lal, B.; Sabil, K.M. Hydrate dissociation condition measurement of CO$_2$—Rich mixed gas in the presence of methanol/ethylene glycol and mixed methanol/ethylene glycol + electrolyte aqueous solution. *J. Chem. Eng. Data* **2014**, *59*, 3920–3926. [CrossRef]

14. Khan, M.S.; Lal, B.; Shariff, A.M.; Mukhtar, H. Ammonium hydroxide ILs as dual-functional gas hydrate inhibitors for binary mixed gas (carbon dioxide and methane) hydrates. *J. Mol. Liq.* **2019**, *274*, 33–44. [CrossRef]

15. Qasim, A.; Khan, M.S.; Lal, B.; Shariff, A.M. Phase equilibrium measurement and modeling approach to quaternary ammonium salts with and without monoethylene glycol for carbon dioxide hydrates. *J. Mol. Liq.* **2019**, *282*, 106–114. [CrossRef]

16. Cha, M.; Shin, K.; Seo, Y.; Shin, J.Y.; Kang, S.P. Catastrophic growth of gas hydrates in the presence of kinetic hydrate inhibitors. *J. Phys. Chem. A* **2013**, *117*, 13988–13995. [CrossRef] [PubMed]

17. Khan, M.S.; Cornelius, B.B.; Lal, B.; Bustam, M.A. Kinetic assessment of tetramethyl ammonium hydroxide (ionic liquid) for carbon dioxide, methane and binary mix gas hydrates. In *Recent Advances in Ionic Liquids*; Rahman, M.M., Ed.; IntechOpen: London, UK, 2018; pp. 159–179. ISBN 978-1-78984-118-3.

18. Karaaslan, U.; Parlaktuna, M. Kinetic inhibition of methane hydrate by polymers. *ACS Div. Fuel Chem. Prepr.* **2002**, *47*, 355–358.

19. Xiao, C.; Adidharma, H. Dual function inhibitors for methane hydrate. *Chem. Eng. Sci.* **2009**, *64*, 1522–1527. [CrossRef]

20. Peng, X.; Hu, Y.; Liu, Y.; Jin, C.; Lin, H. Separation of ionic liquids from dilute aqueous solutions using the method based on CO^2 hydrates. *J. Nat. Gas. Chem.* **2020**, *19*, 81–85.

21. Sabil, K.M.; Nashed, O.; Lal, B.; Ismail, L.; Japper-Jaafar, A. Experimental investigation on the dissociation conditions of methane hydrate in the presence of imidazolium-based ionic liquids. *J. Chem. Thermodyn.* **2015**, *84*, 7–13. [CrossRef]

22. Khan, M.S.; Lal, B.; Bustam, M.A. Gas Hydrate Inhibitors. In *Chemical Additives for Gas Hydrates, Green Energy and Technology*; Springer: Cham, Switzerland, 2020; ISBN 978-3-030-30749-3.

23. Tariq, M.; Rooney, D.; Othman, E.; Aparicio, S.; Atilhan, M.; Khraisheh, M. Gas Hydrate Inhibition: A Review of the Role of Ionic Liquids. *Ind. Eng. Chem. Res.* **2014**, *53*, 17855–17868. [CrossRef]

24. Nashed, O.; Sabil, K.M.; Lal, B.; Ismail, L.; Jaafar, A.J. Study of 1-(2-Hydroxyethyle) 3-methylimidazolium halide as thermodynamic inhibitors. *Appl. Mech. Mater.* **2014**, *625*, 337–340. [CrossRef]

25. Avula, V.R.; Gardas, R.L.; Sangwai, J.S. Modeling of methane hydrate inhibition in the presence of green solvent for offshore oil and gas pipeline. *Int. Soc. Offshore Polar Eng.* **2014**, *3*, 49–54.

26. Rufford, T.E.; Smart, S.; Watson, G.C.Y.; Graham, B.F.; Boxall, J.; Diniz da Costa, J.C.; May, E.F. The removal of CO_2 and N_2 from natural gas: A review of conventional and emerging process technologies. *J. Pet. Sci. Eng.* **2012**, *94*, 123–154. [CrossRef]

27. Nazari, K.; Ahmadi, A.N. A thermodynamic study of methane hydrate formation in the presence of [Bmim][Bf 4] and [Bmim][Ms] ionic liquids. In Proceedings of the 7th Intenational Confrence on Gas Hydrates (ICGH) 2011, Edinbrugh, UK, 17–21 July 2011; p. 9.

28. Nashed, O.; Dadebayev, D.; Khan, M.S.M.S.; Bavoh, C.B.C.B.; Lal, B.; Shariff, A.M. Experimental and modelling studies on thermodynamic methane hydrate inhibition in the presence of ionic liquids. *J. Mol. Liq.* **2018**, *249*, 886–891. [CrossRef]

29. Bavoh, C.B.; Partoon, B.; Keong, L.K.; Lal, B.; Wilfred, C.D. Eeffect of 1-ethyl-3-methylimidazolium chloride and polyvinylpyrrolidone on kineticss of carbon dioxide hydrates. *Int. J. Appl. Chem.* **2016**, *12*, 6–11.

30. Bavoh, C.B.; Lal, B.; Khan, M.S.; Osei, H.; Ayuob, M. Combined Inhibition Effect of 1-Ethyl-3-methy-limidazolium Chloride + Glycine on Methane Hydrate. *J. Phys. Conf. Ser.* **2018**, *1123*, 012060. [CrossRef]

31. Cha, J.H.; Ha, C.; Kang, S.P.; Kang, J.W.; Kim, K.S. Thermodynamic inhibition of CO_2 hydrate in the presence of morpholinium and piperidinium ionic liquids. *Fluid Phase Equilib.* **2016**, *413*, 75–79. [CrossRef]

32. Keshavarz, L.; Javanmardi, J.; Eslamimanesh, A.; Mohammadi, A.H. Experimental measurement and thermodynamic modeling of methane hydrate dissociation conditions in the presence of aqueous solution of ionic liquid. *Fluid Phase Equilib.* **2013**, *354*, 312–318. [CrossRef]

33. Shen, X.; Shi, L.; Long, Z.; Zhou, X.; Liang, D. Experimental study on the kinetic effect of N-butyl-N-methylpyrrolidinium bromide on CO2 hydrate. *J. Mol. Liq.* **2016**, *223*, 672–677. [CrossRef]

34. Kim, K.-S.; Kang, J.W.; Kang, S.-P. Tuning ionic liquids for hydrate inhibition. *Chem. Commun.* **2011**, *47*, 6341–6343. [CrossRef]

35. Khan, M.S.; Lal, B.; Partoon, B.; Kok, L.; Azmi, B. Experimental evaluation of a novel thermodynamic inhibitor for CH4 and CO2 hydrates. *Procedia Eng.* **2016**, *148*, 932–940. [CrossRef]

36. Khan, M.S.; Lal, B.; Bavoh, C.B.; Keong, L.K.; Bustam, A. Influence of ammonium based compounds for gas hydrate mitigation: A short review. *Indian J. Sci. Technol.* **2017**, *10*, 1–6. [CrossRef]

37. Nashed, O.; Koh, J.C.H.; Lal, B. Physical-chemical properties of aqueous TBAOH solution for gas hydrates promotion. *Procedia Eng.* **2016**, *148*, 1351–1356. [CrossRef]

38. Eslamimanesh, A. Thermodynamic Studies on Semi-Clathrate Hydrates of TBAB + Gases Containing Carbon Dioxide. Ph.D. Thesis, Mines ParisTech—Université PSL, Paris, France, 2012.

39. Shin, B.S.; Kim, E.S.; Kwak, S.K.; Lim, J.S.; Kim, K.S.; Kang, J.W. Thermodynamic inhibition effects of ionic liquids on the formation of condensed carbon dioxide hydrate. *Fluid Phase Equilib.* **2014**, *382*, 270–278. [CrossRef]

40. Khan, M.S.; Partoon, B.; Bavoh, C.; Lal, B.; Mellon, N.B. Influence of tetramethylammonium hydroxide on methane and carbon dioxide gas hydrate phase equilibrium conditions. *Fluid Phase Equilib.* **2017**, *440*, 1–8. [CrossRef]

41. Tariq, M.; Connor, E.; Thompson, J.; Khraisheh, M.; Atilhan, M.; Rooney, D. Doubly dual nature of ammonium-based ionic liquids for methane hydrates probed by rocking-rig assembly. *RSC Adv.* **2016**, *6*, 23827–23836. [CrossRef]

42. Khan, M.S.; Lal, B.; Keong, L.K.; Ahmed, I. Tetramethyl ammonium chloride as dual functional inhibitor for methane and carbon dioxide hydrates. *Fuel* **2019**, *236*, 251–263. [CrossRef]

43. Anantharaj, R.; Banerjee, T. Phase behaviour of 1-ethyl-3-methylimidazolium thiocyanate ionic liquid with catalytic deactivated compounds and water at several temperatures: Experiments and theoretical predictions. *Int. J. Chem. Eng.* **2011**, *2011*, 1–13. [CrossRef]

44. Diedenhofen, M.; Klamt, A. COSMO-RS as a tool for property prediction of IL mixtures—A review. *Fluid Phase Equilib.* **2010**, *294*, 31–38. [CrossRef]

45. Tumba, K.; Reddy, P.; Naidoo, P.; Ramjugernath, D.; Eslamimanesh, A.; Mohammadi, A.H.; Richon, D. Phase equilibria of methane and carbon dioxide clathrate hydrates in the presence of aqueous solutions of tributylmethylphosphonium methylsulfate ionic liquid. *J. Chem. Eng. Data* **2011**, *56*, 3620–3629. [CrossRef]

46. Sami, N.A.; Das, K.; Sangwai, J.S.; Balasubramanian, N. Phase equilibria of methane and carbon dioxide clathrate hydrates in the presence of (methanol + MgCl2) and (ethylene glycol + MgCl2) aqueous solutions. *J. Chem. Thermodyn.* **2013**, *65*, 925–928. [CrossRef]

47. Partoon, B.; Sabil, K.M.; Roslan, H.; Lal, B.; Keong, L.K. Impact of acetone on phase boundary of methane and carbon dioxide mixed hydrates. *Fluid Phase Equilib.* **2016**, *412*, 51–56. [CrossRef]

48. Nashed, O.; Partoon, B.; Lal, B.; Sabil, K.M.; Shariff, A.M. Review the impact of nanoparticles on the thermodynamics and kinetics of gas hydrate formation. *J. Nat. Gas. Sci. Eng.* **2018**, *55*, 452–465. [CrossRef]

49. Bavoh, C.B.; Lal, B.; Ben-Awuah, J.; Khan, M.S.; Ofori-Sarpong, G. Kinetics of mixed amino acid and ionic liquid on CO2 hydrate formation. *IOP Conf. Ser. Mater. Sci. Eng.* **2019**, *495*. [CrossRef]

50. Khan, M.S.; Liew, C.S.; Kurnia, K.A.; Cornelius, B.; Lal, B. Application of COSMO-RS in Investigating Ionic Liquid as Thermodynamic Hydrate Inhibitor for Methane Hydrate. *Procedia Eng.* **2016**, *148*, 862–869. [CrossRef]

51. Sowa, B.; Zhang, X.H.; Hartley, P.G.; Dunstan, D.E.; Kozielski, K.A.; Maeda, N. Formation of ice, tetrahydrofuran hydrate, and methane/propane mixed gas hydrates in strong monovalent salt solutions. *Energy Fuels* **2014**, *11*, 6877–6888. [CrossRef]

52. Zieliński, R.; Ikeda, S.; Nomura, H.; Kato, S. Effect of temperature on micelle formation in aqueous solutions of alkyltrimethylammonium bromides. *J. Colloid Interface Sci.* **1989**, *129*, 175–184. [CrossRef]

53. Alger, D.B. The effect of temperature on the solubility of gases in liquids. *J. Chem. Educ.* **1992**, *69*, 62. [CrossRef]

54. Nashed, O.; Sabil, K.M.; Ismail, L.; Japper-Jaafar, A.; Lal, B. Mean induction time and isothermal kinetic analysis of methane hydrate formation in water and imidazolium based ionic liquid solutions. *J. Chem. Thermodyn.* **2017**, *117*, 1–8. [CrossRef]

55. Koh, C.A.; Westacott, R.E.; Zhang, W.; Hirachand, K.; Creek, J.L.; Soper, A.K. Mechanisms of gas hydrate formation and inhibition. *Fluid Phase Equilib.* **2002**, *194*, 143–151. [CrossRef]

56. Bavoh, C.B.; Lal, B.; Keong, L.K.; Binti Jasamai, M.; Binti Idress, M. Synergic Kinetic Inhibition Effect of EMIM-Cl + PVP on CO2 Hydrate Formation. *Procedia Eng.* **2016**, *148*, 1232–1238. [CrossRef]

57. Nguyen, N.N.; Nguyen, A.V. Hydrophobic effect on gas hydrate formation in the presence of additives. *Energy Fuels* **2017**, *31*, 10311–10323. [CrossRef]

58. Sloan, E.D.; Koh, C.A.; Sloan, E.D. *Clathrate Hydrates of Natural Gases*, 3rd ed.; CRC Press Taylor & Francis: Boca Raton, FL, USA, 2008; Volume 87, ISBN 9781420008494.

59. Circone, S.; Stern, L.A.; Kirby, S.H.; Durham, W.B.; Chakoumakos, B.C.; Rawn, C.J.; Rondinone, A.J.; Ishii, Y. CO2 hydrate: Synthesis, composition, structure, dissociation behavior, and a comparison to structure I CH4 hydrate. *J. Phys. Chem. B* **2003**, *107*, 5529–5539. [CrossRef]

60. Sa, J.-H.; Kwak, G.-H.; Han, K.; Ahn, D.; Lee, K.-H. Gas hydrate inhibition by perturbation of liquid water structure. *Sci. Rep.* **2015**, *5*, 11526. [CrossRef] [PubMed]

61. Villano, L.D.; Kommedal, R.; Fijten, M.W.M.; Schubert, U.S.; Hoogenboom, R.; Kelland, M.A. A study of the kinetic hydrate inhibitor performance and seawater biodegradability of a series of poly(2-alkyl-2-oxazoline)s. *Energy Fuels* **2009**, *23*, 3665–3673. [CrossRef]

62. Bhargava, B.L.; Yasaka, Y.; Klein, M.L. Computational studies of room temperature ionic liquid-water mixtures. *Chem. Commun.* **2011**, *47*, 6228–6241. [CrossRef]

63. Oliver, R.C.; Lipfert, J.; Fox, D.A.; Lo, R.H.; Doniach, S.; Columbus, L. Dependence of micelle size and shape on detergent alkyl chain length and head group. *PLoS ONE* **2013**, *8*, e62488. [CrossRef]

64. Kartikawati, N.A.; Safdar, R.; Lal, B.; Mutalib, M.I.B.A.; Shariff, A.M. Measurement and correlation of the physical properties of aqueous solutions of ammonium based ionic liquids. *J. Mol. Liq.* **2018**, *253*, 250–258. [CrossRef]

65. Khan, M.S.; Lal, B.; Keong, L.K.; Sabil, K.M. Experimental evaluation and thermodynamic modelling of AILs alkyl chain elongation on methane riched gas hydrate system. *Fluid Phase Equilib.* **2018**, *473*, 300–309. [CrossRef]

66. Khan, M.S.; Bavoh, C.B.; Partoon, B.; Nashed, O.; Lal, B.; Mellon, N.B. Impacts of ammonium based ionic liquids alkyl chain on thermodynamic hydrate inhibition for carbon dioxide rich binary gas. *J. Mol. Liq.* **2018**, *261*, 283–290. [CrossRef]